Journal of Clinical Immunology (2019) 39:188–194
https://doi.org/10.1007/s10875-019-00604-9

ORIGINAL ARTICLE

Novel Heterogeneous Mutation of TNFAIP3 in a Chinese Patient with Behçet-Like Phenotype and Persistent EBV Viremia

Xiaolong Dong[1] · Luyao Liu[1] · Ying Wang[1] · Xiaotao Yang[2] · Wenjie Wang[1] · Li Lin[1] · Bijun Sun[1] · Jia Hou[1] · Wenjing Ying[1] · Xiaoying Hui[1] · Qinhua Zhou[1] · Danru Liu[1] · Haili Yao[1] · Jinqiao Sun[1] · Xiaochuan Wang[1]

Received: 13 December 2018 / Accepted: 19 February 2019 / Published online: 27 February 2019

Abstract

Purpose Tumor necrosis factor alpha-induced protein 3 (TNFAIP3, A20) is a negative regulator of the nuclear factor-κB (NF-κB) pathway. It has recently been recognized that TNFAIP3 deficiency leads to early onset of autoinflammatory and autoimmune syndrome resembling Behçet's disease. Here, we report a novel mutation in *TNFAIP3* in a Chinese patient, who had Behçet-like phenotype and persistent Epstein-Barr virus (EBV) viremia.

Methods The clinical data were collected. Immunological function was detected. Gene mutation was detected by whole-exome sequencing (WES) and confirmed by Sanger sequencing. mRNA and protein levels were detected in the patient under lipopolysaccharide (LPS) stimulation by real-time PCR and Western blot.

Results The patient is a 13-year-old boy, presenting with intermittent fever for 5 months, who also experienced diffuse lymphadenopathy, arthritis, and recurrent multiple gastrointestinal ulcers. EBV DNA was detected in the serum and peripheral blood mononuclear cells of the patient. The immunological phenotype showed increased proportion of double-negative T cells (CD3+ CD4−CD8−). A novel missense mutation (c.1428G > A) locating at the zinc fingers 2 (ZF2) domain of *TNFAIP3* inherited from his mother was confirmed. Compared with age-matched healthy controls, decrease expression of A20 was observed in the patient. The NF-κB pathway was found to be overactivated, and the synthesis of TNF-α was upregulated in the patient-derived cells. However, cells from the mother showed a milder response to LPS than cells from the patient.

Conclusions The present research indicated that the *TNFAIP3* mutation of c.1428G > A (p.M476I) leads to the reduced suppression of NF-κB activation and accounted for the autoinflammatory phenotype and persistent EBV viremia in the patient.

Keywords TNFAIP3 · NF-κB · autoinflammatory · EBV viremia

Introduction

Monogenic autoinflammatory diseases are characterized by unprovoked episodic or persistent inflammation without evidence of high-titer autoantibodies or antigen-specific T lymphocytes [1]. In recent decades, more than 20 causative genes have been determined to be responsible for immune regulatory disorders, many of which present with fever, systemic inflammation, and organ-specific inflammation [2]. The proteins encoded by these genes play important roles in the regulation of the inflammatory response and are mainly expressed in cells of the innate immune system [3]. Therefore, appropriate mediating mechanisms of innate immune pathways are crucial for avoiding these diseases and can help us devise therapeutic strategies.

The canonical nuclear factor-κB (NF-κB) signaling pathway is the best characterized molecular pathway for triggering immune cell activation by initiating the transcription of numerous pro-inflammatory genes [4]. Excessive activation of NF-κB signaling in multiple cell types has been linked to both human and experimental inflammatory diseases [5]. The A20 protein encoded by *TNFAIP3* is required for preventing spontaneous inflammation and restricting the duration of tumor

Xiaolong Dong and Luyao Liu contributed equally to this work.

✉ Jinqiao Sun
jinqiaosun@fudan.edu.cn

✉ Xiaochuan Wang
xchwang@shmu.edu.cn

[1] Department of Clinical Immunology, Children's Hospital of Fudan University, 399 Wanyuan Road, Shanghai 201102, China

[2] Kunming Children's Hospital Affiliated to Kunming Medical University, Kunming 650000, Yunnan, China

necrosis factor (TNF), Toll-like receptor, interleukin-1 receptor (IL-1R), and nucleotide-binding oligomerization domain containing 2 (NOD2)-induced NF-κB signals [6–9]. A20 terminates the NF-κB activation cascade by removing K63-linked ubiquitin chains and by building K48-linked polyubiquitin chains on key adaptor proteins, which leads to proteasomal degradation.

Loss function of A20 in mice results in severe spontaneous inflammation, cachexia, and premature death [10]. Genetic studies in humans have also revealed the role of *TNFAIP3* in susceptibility to complex genetic autoimmune disorders [11–13]. Germline single nucleotide polymorphisms (SNPs) of *TNFAIP3* have been linked with susceptibility to multiple human diseases, such as systemic lupus erythematosus (SLE) [14], rheumatoid arthritis, psoriasis [15], type 1 diabetes [16], celiac disease [17], and Crohn's disease [18]. The first human disease caused by a high penetrance pathogenic mutation of A20 was reported in 2016, followed by reports of several cases of *TNFAIP3* deficiency [19–23]. Autoimmune phenomena were not prominent in most of the recently described patients with germline A20 mutations, who instead developed an autoinflammatory phenotype resembling Behçet's disease [21, 22].

In the present study, we report a 13-year-old boy, who presented with Behçet's-like phenotype including recurrent fever, gastrointestinal ulcers, and arthritis, was identified as carrying an identical novel *TNFAIP3* mutation inherited from his mother. Functional experiments revealed that the expression of A20 was decreased and NF-κB signaling was overactivated in the cells from the patient.

Method

The study was approved by the Ethics Committee of the Children's Hospital of Fudan University. The patient and his parents provided written informed consent for enrollment in this study.

Routine Evaluation of Immunological Function

IgG, IgA, and IgM were detected by nephelometry as previously reported [24], and IgE was assessed by UniCAP (Pharmacia, Uppsala, Sweden). We used a FACSCalibur flow cytometer (Becton Dickinson, Franklin Lakes, NJ, USA) to analyze the lymphocyte subsets. Whole blood was used for staining lymphocyte surface markers after red cell lysis and for analysis according to a standard multicolor flow cytometric protocol with appropriate fluorochrome-labeled monoclonal antibodies or isotype-matched control antibodies. After being washed twice with PBS, 1×10^4 to 5×10^4 live cells were analyzed by flow cytometry (Becton Dickinson, Franklin Lakes, NJ, USA) using FACSDiva software (BD Biosciences). The following validated antibodies were used for flow cytometry: anti-CD3 (UCHT1), anti-CD8 (RPA-T8), anti-CD27 (M-T271), anti-CD45RA (HI100), anti-CD4 (RPA-T4), anti-TCRαβ (T10B9.1A-31), anti-TCRγδ (B1), anti-CD19 (HIB19), anti-CD24 (ML5), anti-CD38 (HIT2), and anti-IgD (IA6-2) (all from BD Biosciences).

Genetic Analysis

Whole-exome sequencing (WES) and analysis protocols were adapted for genetic analysis. The genomic DNA fragments of the patient and his parents were enriched for sequencing. Enriched DNA samples were indexed and sequenced on a HiSeq 2000 sequencer (Illumina, San Diego, CA). Nucleotide changes observed in more than 5% of aligned reads were identified and reviewed by using NextGENe software (SoftGenetics, State College, PA).

Mutations in *TNFAIP3* were confirmed by using Sanger sequencing. Briefly, genomic DNA was extracted from peripheral blood mononuclear cells (PBMCs) using the Relax Gene Blood DNA System (Tiangen Biotech, Beijing, China). Polymerase chain reaction (PCR) was performed using synthetic oligonucleotide primers to amplify genomic DNA. After an initial denaturation step for 5 min at 95 °C, 35 cycles of amplification were performed as follows: 95 °C for 30 s, 60 °C for 30 s, and 72 °C for 40 s. The final extension was performed at 72 °C for 7 min. After PCR, genomic DNA products were purified using Performa DTR Gel Filtration Cartridges. Then, we directly sequenced the TNFAIP3 gene using ABI Prism BigDye Terminators.

PBMC Isolation and Cell Culture

Venous blood was drawn from three healthy volunteers and the patient. The EDTA-anticoagulated blood was diluted with an equal volume of phosphate-buffered saline (PBS). The diluted blood was carefully added to the top of the Ficoll-Paque Plus (Amersham Pharmacia Biotech, Baie-D'Urfé, Quebec, Canada) and centrifuged at 2000 rpm at room temperature to separate the plasma from the PBMC fraction. After being washed twice in PBS, the PBMCs were cultured in RPMI 1640 supplemented with 10% FCS at a density of 1×10^6 cells/mL. Stimulation was achieved by adding ultrapure *E. coli* LPS (Sigma-Aldrich, USA) to the cell culture at a final concentration of 100 ng/mL. After incubation in a 12-well plate at 37 °C in 5% CO_2 for 24 h, the cells were harvested for subsequent experiments.

Quantitative PCR

RNA was extracted using RNAiso Plus Reagent (TaKaRa, Japan). cDNA was synthesized from 500 ng of total RNA using Transcript RT Master Mix (Takara, Japan) following

the manufacturer's instructions. Real-time RT-PCR was performed using Takara SYBR Fast qPCR Mix (Takara, Japan) on a LightCycler 480 Instrument II (Roche, Switzerland). The primer sequences were as follows: A20 (Forward): 5′-GAGC AACTGAGATCGAGCCA-3′, A20 (Reverse): 5′-TGGT TGGGATGCTGACACTC-3′, TNF-α (Forward): 5′-TCTC TCCCCTGGAAAGGACA-3′, TNF-α (Reverse): 5′-AGAG GCTGAGGAACAAGCAC-3′. The reactions included 2 μL of cDNA, 10 μL of SYBR Green Mix, 0.8 μL of each of forward and reverse primers, and 6.4 μL of ddH2O. The thermocycler conditions were 95 °C for 30 s, followed by 40 cycles at 95 °C for 5 s, 60 °C for 20 s, and 72 °C for 20 s. Melting curve analysis was performed at the end of expression analysis using the following conditions: 55 °C for 60 s, followed by 81 cycles starting at 55 °C for 10 s with a 0.5 °C increase with each cycle. The qPCR data were analyzed using the $2^{-\Delta\Delta CT}$ method [25]. The β-actin gene was used as an inner reference, and the expression of *TNFAIP3* was quantified relative to the mRNA levels in the unstimulated cells from healthy controls. The experiments were performed with three replicates, and the results were analyzed using Student's *t* test or a one-way analysis of variance (ANOVA) and Duncan's test using SPSS 20 (IBM Corporation, USA).

Western Blot

Cytoplasmic and nuclear proteins were extracted using NE-PER™ Nuclear and Cytoplasmic Extraction Reagents (Thermo Fisher Scientific, USA) following the manufacturer's instructions. Equal amounts of cytoplasmic or nuclear extracts were separated on 12% SDS polyacrylamide gels and transferred to PVDF membranes. Blots were probed with primary antibodies against A20, NF-κB p65, β-actin, or histone H3 (Cell Signaling Technology, Beverly, MA). Primary antibodies were detected with horseradish peroxidase-conjugated secondary antibody. Visualization was conducted using an ECL peroxidase substrate.

Results

Case Presentation

A 13-year-old Chinese boy presented with intermittent fever for 5 months with unknown origin. In the course of fever, he had rashes on the skin and increased levels of erythrocyte sedimentation rate (55 mm/h). Treatment with antibiotics was not effective. The patient presented with diffuse lymphadenopathy, especially bilateral cervical lymphadenopathy accompanied by apparent tenderness pain. Mild hepatomegaly was also observed in the patient, and the size of the liver measured infracostal 2 cm. The patient also presented with Behçet-like phenotype. Recurrent tonsillitis occurred since 2 years old, approximately 5 to 6 times per year. Joint pains were noted during fever. Type B ultrasound revealed that the synovial membrane was thickened in the joints of the right wrist, hips, knees, and ankles accompanied by joint capsule effusion (Fig. 1a). He experienced recurrent oral ulcers and long-term constipation. Multiple ulcers (colonic and small intestine ulcers, antral gastric ulcers, and duodenal ulcers) were identified by endoscopy (Fig. 1b). Furthermore, he suffered from persistent Epstein-Barr virus (EBV) infection (Table 1). EBV DNA was detected in the serum (2.80E+03 copies/mL) and peripheral blood mononuclear cells (7.81E+06 copies/mL) by viral DNA PCR. Blood serum/chemical analysis revealed elevated levels of globulin (31.9 g/L) and glucose (7.5 mmol/L). Measurements of autoantibodies, including anti-proliferating cell nuclear antigen antibody (PCNA), anti-mitochondrial antibody (AMA), anti-double-stranded DNA (dsDNA) antibody, and anti-histone antibody, were all negative. He received acyclovir and prednisolone treatment, with a transient improvement of clinical symptoms.

Genetic Analysis

WES was performed on the present patient and his parents. The patient and his mother carried heterozygous c.1428G > A missense mutations of *TNFAIP3*, both of which were confirmed by Sanger sequencing (Fig. 2a). This mutation caused amino acid conversion of p.M476I in the zinc finger 2 (ZF2) domain of A20, and it has not been reported in any database, including the National Center for Biotechnology Information and Human Genetic Variation Database (Fig. 2b).

Immunological Features

The immunological characteristics of the patient are listed in Table 2. We observed that the proportion of double-negative T cells (DNT) (CD3+CD4−CD8−) was increased (58.8%); however, the proportion of TCRαβ + DNT cells was within normal limits (0.3%). The patient showed an increased proportion of effector memory cytotoxic T cells (CD8+CD45RA−CD27−) (36.1%; reference range 1.24–24.52%). Reduced numbers of helper T (Th) cells (CD3+CD4+) (24.36%; reference range 29–36%) and cytotoxic T cells (CD3+CD8+) (14.8%; reference range 24–34%) were detected in the patient. The B lymphocyte subpopulations and the immunoglobulin (Ig)G and IgM levels were normal. However, increased IgA and IgE levels were detected.

Expression of A20 in the Patient

Real-time PCR and Western blot analyses were performed to determine whether the mutation influenced the expression of A20 under the condition of LPS stimulation in patient-derived cells. The results showed that the mRNA accumulation of

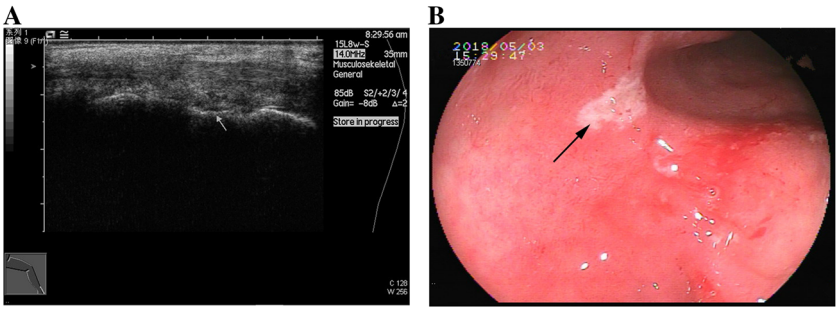

Fig. 1 Clinical data of the patient. **a** Type B ultrasound revealed that the synovial membrane was thickened in the ankle joints, accompanied by joint capsule effusion. **b** Gastrointestinal endoscopy showing ulcers

TNFAIP3 increased 2.96 times after LPS treatment in cells from healthy controls. In the PBMCs of the patient and his mother, the *TNFAIP3* expression was also upregulated after LPS stimulation compared with the unstimulated PBS treatment; however, the mRNA levels in the patient and his mother were dramatically decreased compared with the healthy controls in both the unstimulated and LPS-stimulated treatments. Furthermore, *TNFAIP3* expression was slightly greater in the cells from the mother than in those from the patient (Fig. 3a). Western blot analysis showed that the A20 protein level was upregulated in LPS-stimulated treatment compared with unstimulated PBS treatment in PBMCs from healthy controls, while in the patient- and mother-derived cells, LPS stimulation had no significant effect on the expression of the A20 protein. (Fig. 3b).

NF-κB Pathway Activation in Patient-Derived Cells

Upon cell stimulation, the freed NF-κB molecular subunits, for example, p50 and p65, translocate into the nucleus to regulate the expression of multiple target genes [26]. In the present study, the influence of the A20 mutation was assessed by performing immunoblotting. The results showed that in the health control and mother, the expression level of total p65 protein was almost equal in whole-cell lysates from PBS and LPS treatments and p65 level was decreased in cytoplasm whereas the phospho-p65 (p-p65) was increased in nucleus after LPS stimulation. In the patient, the p65 levels of whole-cell lysates and cytoplasm were slightly increased after LPS stimulation and the p-p65 level was significantly increased after stimulation. Furthermore, in the unstimulated cell sets, more p65 molecules were kept in the cytoplasm of health control than in the patient and mother, while the p-p65 level in nuclei was significantly higher in the patients and mother than in the health control. These results indicated that NF-κB signaling was active even without stimulation in the patient (Fig. 4a). As a consequence, in the unstimulated cells of the patient and his mother, the TNF-α levels were 9.71 and 4.3 times greater than in the healthy controls, respectively. In addition, the expression of TNF-α was also significantly greater in the patient and mother than in the healthy control group after LPS stimulation (Fig. 4b).

Discussion

There is much evidence indicating that A20 plays an important role in autoinflammation. Both biallelic and monoallelic inactivation of A20 can lead to activation of NF-κB, and the mRNA levels of target genes modulated by NF-κB molecules were upregulated in the liver of A20 haploinsufficient mice [27]. A number of studies have indicated that human *TNFAIP3* polymorphisms are associated with certain diseases [28]. In addition, the first research on heterozygous mutations of *TNFAIP3* in six unrelated families with early-onset systemic inflammation was conducted in 2016 [19]. Later, some other cases were identified and reported. These findings illustrated the importance of *TNFAIP3* in the resolution of inflammation.

The C-terminal domain of the A20 protein contains seven zinc fingers (ZFs), and early studies showed that ZFs are essential for inhibiting NF-κB signaling, especially ZF4 and ZF7 [29]. Some researchers have the opinion that the other five ZFs of A20 may have important functions complementary to those of ZF4 and ZF7 [30]. In the present study, the mutation site in the patient is located at the coding region of ZF2, and our results have proven this viewpoint since the translocation of p65 into the nucleus significantly increased in the patient-derived cells. As a consequence, the expression of the TNF-α gene was upregulated. Furthermore, we also observed abnormal

Table 1 EBV DNA copies of the patient

	2-9-2018	4-25-2018	5-28-2018	Reference
Blood serum (copies/mL)	2.54E+03	2.38E+03	2.80E+03	<lower detection limit
Peripheral blood mononuclear cells (copies/mL)	6.89E+05	3.76E+06	7.81E+06	<lower detection limit

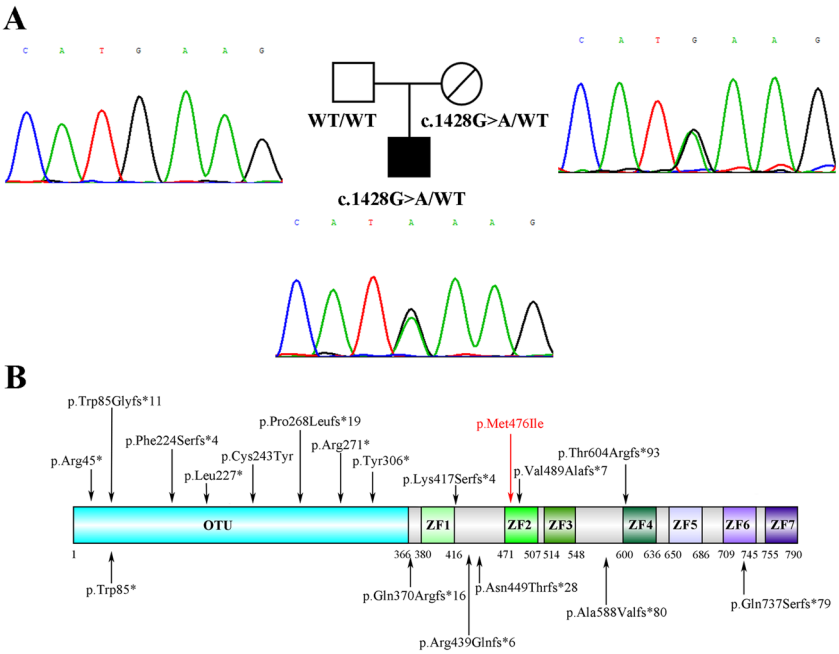

Fig. 2 Genetic analysis of the patient. **a** Family tree and confirmation of a mutation in *TNFAIP3* by Sanger sequencing. **b** Schematic protein structure of TNFAIP3 (A20). The location of the present mutation is represented with a red arrow and previously reported mutations were represented in black. OUT, OUT-like cysteine protease domain; ZF, zinc finger domain

Table 2 Immunological characteristics of the patient

Lymphocyte subpopulation	*N*/total% (AC/μL)	Reference value %
T cells	78.57 (3576) ↑	64–73
Th cells (CD3+CD4+)	24.36 (1108.97) ↓	29–36
Naive Th cells (CD4+CD45RA+CD27+)	42.9	33.02–76.40
Central memory Th cells (CD4+CD45RA−CD27+)	44.7	19.22–52.82
Effector memory Th cells (CD4+CD45RA−CD27−)	12	2.52–19.80
Cytotoxic T cells (CD3+CD8+)	14.8 (673.42)↓	24–34
Naive cytotoxic T cells (CD8+CD45RA+CD27+)	45.6	26.84–80.28
Central memory cytotoxic T cells (CD8+CD45RA−CD27+)	15.2	7.58–41.62
Effector memory cytotoxic T cells (CD8+CD45RA−CD27−)	36.1 ↑	1.24–24.52
Terminal effector memory cytotoxic T cells (CD8+CD45RA+CD27−)	3	1.28–45.30
Double-negative T cells (CD3+CD4−CD8−)	58.8 ↑	0.37–4.16
TCRαβ + double-negative T cells	0.3	0.61–2.31
TCRγδ + double-negative T cells	50.7 ↑	6.55–20.28
B cells		
B cell counts (CD19+)	19 (864.67)	14–21
Naive B cells (CD19+IgD+CD27−)	83.3	42.82–84.54
Memory B cells (CD19+IgD−CD27+)	5.9	4.44–32.26
Transitional B cells (CD19+CD24++CD38++)	1.2	0.54–11.82
NK cells		
NK cell counts (CD16+CD56+)	0.81 (36.97) ↓	11–23
Immunoglobulin		
IgG (g/L)	13.7	6.98–14.26
IgA (g/L)	2.87 ↑	0.92–2.5
IgM (g/L)	1.57	0.56–2.16
IgE (KU/L)	1458.05 ↑	< 100

Th cell, helper T cell; TCR, T cell receptor; Ig, immunoglobulins; AC, absolute count

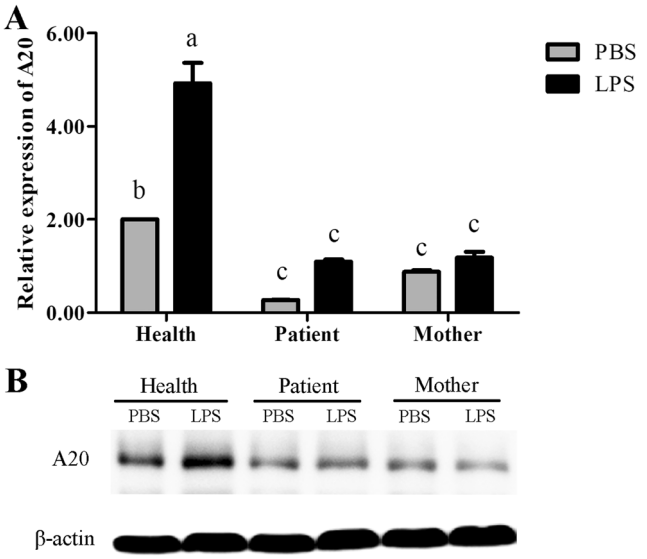

Fig. 3 A20 expression in the patient. **a** mRNA accumulation of *TNFAIP3* in PBMCs derived from the healthy controls and the patient after stimulation with LPS. **b** The protein level of A20 in PBMCs of the patient. PBS, unstimulated treatment; LPS, stimulated with LPS. Normalized target gene mRNA accumulation is reported relative to the mRNA accumulation in the PBS treatment of healthy controls, which was set to 1. All error bars represent the S.E. of the mean of three independent replicates. Different letters indicate a significant difference in mRNA accumulation among the treatments ($P < 0.05$, Duncan's test)

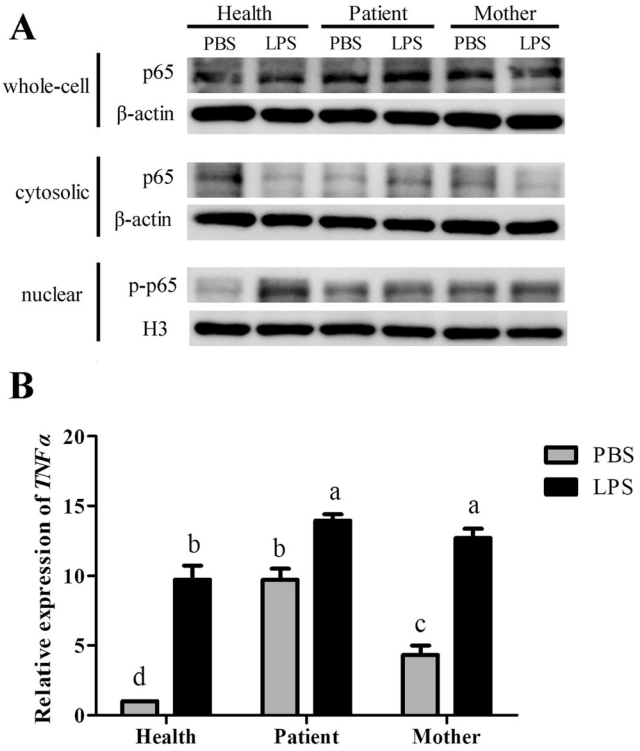

Fig. 4 NF-κB activation in the patient. **a** The protein levels of p65/p-p65 in whole-cell lysates, cytosolic fractions, and nuclear extracts were measured by Western blot analysis. **b** mRNA accumulation of the *TNF-α* gene in the cells derived from the healthy controls and the patient after LPS stimulation. PBS, unstimulated treatment; LPS, stimulated with LPS. Normalized target gene mRNA accumulation is reported relative to the mRNA accumulation in the PBS treatment of the healthy controls, which was set to 1. All error bars represent the S.E. of the mean of three independent replicates. Different letters indicate a significant difference in mRNA accumulation among the treatments ($P < 0.05$, Duncan's test)

NF-κB activation in cells from the mother, who also encountered recurrent fever at a young age and suffered from continuous, persistent oral ulcers. The symptom of the mother was much milder than the patient. This was reasonable since autosomal-dominant-inheritance diseases often show variable penetrance among the different members in the same family. Previous research investigating patient with A20 haploinsufficiency also proved the different penetrance within the patients who had the identical genotype. This kind of difference in penetrance may be attributed to the effects of other genetic and environmental factors [31].

Among all of the reported patients with A20 mutations, most of them had oral and genital ulcers, and most cases exhibited arthralgia, arthritis, or both [19–23]. Consistent with previous reports, the present case also showed oral ulcers and polyarthralgia. A20 is a common genetic target in B-lineage lymphomas and is frequently inactivated in mucosa-associated tissue lymphoma and Hodgkin's lymphoma [32, 33]. This may be the reason leading to lymphoproliferation in A20-deficient patients. A dramatically increased proportion of DNT (58.8%) was observed in our patient. A previously reported *TNFAIP3*-mutant patient also exhibited a high proportion of DNT, which was 15.4% of the total lymphocytes [23]. Lymphoproliferation and increased DNT count are both the most common phenotypes of autoimmune lymphoproliferative syndrome (ALPS). However, the present patient showed skin rashes, which was similar to some A20-deficient patients reported previously. Extensive clinical experience indicated that skin involvement is relatively rare in patients with typical ALPS or ALPS-like diseases. This phenotype might help identify *TNFAIP3* mutations in patients.

This is the first time that EBV viremia was found in the patient with a heterozygous germline mutation of *TNFAIP3*. In fact, A20 alteration is seen in certain EBV-related lymphomas, and A20 inactivation may contribute to the pathogenesis of these diseases [34]. However, none of the reported A20-deficient patients have developed lymphomas or other malignancies. The relationship between the loss of function of A20 and EBV susceptibility needs to be further studied.

Acknowledgments This study was supported by the National Natural Science Foundation of China (81471482), the Science and Technology Commission of Shanghai Municipality (14411965400), the Shanghai Hospital Development Center (SHDC12016228), and Children's Hospital of Fudan University Funding (EK1125180110, EK112520180202). Many thanks to the patient and his parents.

Compliance with Ethical Standards

Conflict of Interest The authors declare that they have no conflict of interest.

Publisher's Note Springer Nature remains neutral with regard to jurisdictional claims in published maps and institutional affiliations.

References

1. Kastner DL, Aksentijevich I, Goldbachmansky R. Autoinflammatory disease reloaded: a clinical perspective. Cell. 2010;140(6):784–90.
2. Jesus AAD, Goldbach-Mansky R. Monogenic autoinflammatory diseases: concept and clinical manifestations. Clin Immunol. 2013;147(3):155–74.
3. Russo RAG, Brogan PA. Monogenic autoinflammatory diseases. Rheumatology. 2014;53(11):1927–39.
4. Baltimore D. NF-κB is 25. Nat Immunol. 2011;12(8):683–5.
5. Rui L, Schmitz R, Ceribelli M, Staudt LM. Malignant pirates of the immune system. Nat Immunol. 2011;12(10):933–40.
6. Wertz IE, O'Rourke KM, Zhou H, Eby M, Aravind L, Seshagiri S, et al. De-ubiquitination and ubiquitin ligase domains of A20 downregulate NF-B signalling. Nature. 2004;430(7000):694–9.
7. David LBDL, Emre ETEE, Eric GLEG, R-C RCA, Matthew TWMT, Colleen TC, et al. The ubiquitin-modifying enzyme A20 is required for termination of Toll-like receptor responses. Nat Immunol. 5:1052–60 Nature Immunology. 2005;6(1):114.
8. Hitotsumatsu O, Ahmad RC, Tavares R, Wang M, Philpott D, Turer EE, et al. The ubiquitin-editing enzyme A20 restricts nucleotide-binding oligomerization domain containing 2-triggered signals. Immunity. 2008;28(3):381–90.
9. Jäättelä M, Mouritzen H, Elling F, Bastholm L. A20 zinc finger protein inhibits TNF and IL-1 signaling. J Immunol. 1996;156(3):1166–73.
10. Lee EG, Boone DL, Chai S, Libby SL, Chien M, Lodolce JP, et al. Failure to regulate TNF-induced NF-κB and cell death responses in A20-deficient mice. Science. 2000;289(5488):2350–4.
11. Musone SL, Taylor KE, Nititham J, Chu C, Poon A, Liao W, et al. Sequencing of TNFAIP3 and association of variants with multiple autoimmune diseases. Genes Immun. 2011;12(3):176–82.
12. Lee YH, Bae SC, Choi SJ, Ji JD, Song GG. Associations between TNFAIP3 gene polymorphisms and rheumatoid arthritis: a meta-analysis. Inflamm Res. 2012;61(6):635–41.
13. Zhu L, Wang L, Wang X, Zhou L, Liao Z, Xu L, et al. Characteristics of A20 gene polymorphisms and clinical significance in patients with rheumatoid arthritis. J Transl Med. 2015;13(1):215.
14. Musone SL, Taylor KE, Lu TT, Nititham J, Ferreira RC, Ortmann W, et al. Multiple polymorphisms in the TNFAIP3 region are independently associated with systemic lupus erythematosus. Nat Genet. 2008;40(9):1062–4.
15. Elsby LM, Orozco G, Denton J, Worthington J, Ray DW, Donn RP. Functional evaluation of TNFAIP3 (A20) in rheumatoid arthritis. Clin Exp Rheumatol. 2010;28(5):708–14.
16. Fung EY, Smyth DJ, Howson JM, Cooper JD, Walker NM, Stevens H, et al. Analysis of 17 autoimmune disease-associated variants in type 1 diabetes identifies 6q23/TNFAIP3 as a susceptibility locus. Genes Immun. 2009;10(2):188–91.
17. Eyre S, Hinks A, Bowes J, Flynn E, Martin P, Wilson AG, et al. Overlapping genetic susceptibility variants between three autoimmune disorders: rheumatoid arthritis, type 1 diabetes and coeliac disease. Arthritis Res Ther, 12,5(2010-09-20). 2010;12(5):R175-R.
18. Burton PR, Clayton DG, Cardon LR, Craddock N, Deloukas P, Duncanson A, et al. Genome-wide association study of 14,000 cases of seven common diseases and 3,000 shared controls. Nature. 2007;447(7145):661–78.
19. Zhou Q, Wang H, Schwartz DM, Stoffels M, Park YH, Zhang Y, et al. Loss-of-function mutations in TNFAIP3 leading to A20 haploinsufficiency cause an early-onset autoinflammatory disease. Nat Genet. 2016;48(1):67–73.
20. Duncan CJA, Dinnigan E, Theobald R, Grainger A, Skelton AJ, Hussain R, et al. Early-onset autoimmune disease due to a heterozygous loss-of-function mutation in TNFAIP3 (A20). Ann Rheum Dis. 2017. https://doi.org/10.1136/annrheumdis-2016-210944.
21. Ohnishi H, Kawamoto N, Seishima M, Ohara O, Fukao T. A Japanese family case with juvenile onset Behçet's disease caused by TNFAIP3 mutation. Allergol Int. 2017;66(1):146–8.
22. Tomonari S, Naoe K, Norimoto K, Keiko K, Yusuke T, Naoko N, et al. Novel heterozygous C243Y A20/TNFAIP3 gene mutation is responsible for chronic inflammation in autosomal-dominant Behçet's disease. RMD Open. 2016;2(1):e000223.
23. Takagi M, Ogata S, Ueno H, Yoshida K, Yeh T, Hoshino A, et al. Haploinsufficiency of TNFAIP3 (A20) by germline mutation is involved in autoimmune lymphoproliferative syndrome. J Allergy Clin Immunol. 2017;139(6):1914–22.
24. Sun J, Ying W, Liu D, Hui X, Yu Y, Wang J, et al. Clinical and genetic features of 5 Chinese patients with X-linked lymphoproliferative syndrome. Scand J Immunol. 2013;78(5):463–7.
25. Livak KJ, Schmittgen TD. Analysis of relative gene expression data using real-time quantitative PCR and the 2(-Delta Delta C(T)) method. Methods. 2001;25(4):402–8.
26. Hayden MS, Ghosh S. Signaling to NF-kappaB. Genes Dev. 2004;18(18):2195–224.
27. Hymowitz SG, Wertz IE. A20: from ubiquitin editing to tumour suppression. Nat Rev Cancer. 2010;10(5):332–41.
28. Catrysse L, Vereecke L, Beyaert R, Van LG. A20 in inflammation and autoimmunity. Trends Immunol. 2014;35(1):22–31.
29. Song HY, Rothe M, Goeddel DV. The tumor necrosis factor-inducible zinc finger protein A20 interacts with TRAF1/TRAF2 and inhibits NF-kappaB activation. Proc Natl Acad Sci U S A. 1996;93(13):6721–5.
30. Ma A, Malynn BA. A20: linking a complex regulator of ubiquitylation to immunity and human disease. Nat Rev Immunol. 2012;12(11):774–85.
31. Kadowaki T, Ohnishi H, Kawamoto N, Hori T, Nishimura K, Kobayashi C, et al. Haploinsufficiency of A20 causes autoinflammatory and autoimmune disorders. J Allergy Clin Immunol. 2018;141(4):1485–8.
32. Nomoto J, Hiramoto N, Kato M, Sanada M, Maeshima AM, Taniguchi H, et al. Deletion of the TNFAIP3/A20 gene detected by FICTION analysis in classical Hodgkin lymphoma. BMC Cancer, 12,1(2012-10-05). 2012;12(1):457.
33. Kato M, Sanada M, Kato I, Sato Y, Takita J, Takeuchi K, et al. Frequent inactivation of A20 in B-cell lymphomas. Nature. 2009;459(7247):712–6.
34. Ando M, Sato Y, Takata K, Nomoto J, Nakamura S, Ohshima K, et al. A20 (TNFAIP3) deletion in Epstein-Barr virus-associated lymphoproliferative disorders/lymphomas. PLoS One. 2013;8(2):e56741.